Jurnal Teknologi

Full Paper

DESIGNING TECHNO-ECONOMIC OFF-GRID PHOTOVOLTAIC SYSTEM USING AN IMPROVED DIFFERENTIAL EVOLUTION ALGORITHM

Seth Bedu Rockson[a*], Madihah Md Rasid[b], Mohd Shafiq Anuar[c], Siti Maherah Hussin[b], Norzanah Rosmin[b], Norjulia Mohamad Nordin[b], Michael Gyan[d]

[a]Department of Electrical Engineering, Koforidua Technical University, Koforidua-Ghana
[b]Faculty of Electrical Engineering, Universiti Teknologi Malaysia, 81310 UTM Johor Bahru, Johor ,Malaysia
[c]Project Lebuhraya Usahasama Berhad, Malaysia
[d]Department of Physics, University of Education Winneba, Ghana

Article history
Received
20 February 2022
Received in revised form
5 April 2023
Accepted
30 April 2023
Published Online
25 June 2023

*Corresponding author
madihahmdrasid@utm.my

Graphical abstract

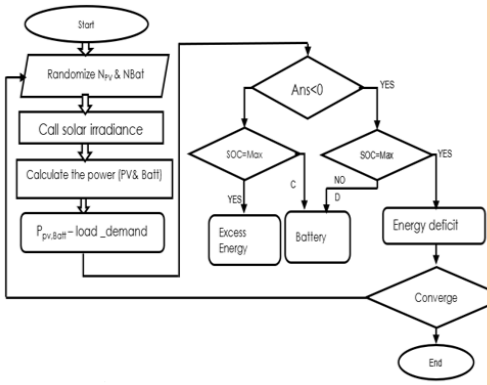

Abstract

Conventional power generation is one of the main contributors to the phenomenon of the greenhouse effect. This has led to a diversification of electricity sources including environmentally friendly energy sources such as solar energy. Off-grid PV systems have gained some traction due to their cost-effectiveness for rural communities. However, the intermittent nature of solar is the main challenge to developing the off-grid PV system. Moreover, the high capital cost of PV systems as well as the storage batteries becomes the main concern for all PV users. Thus, this study aims to optimize the size of the PV system and battery simultaneously and design a cost-effective off-grid photovoltaic system considering various aspects such as battery power, solar irradiance, and PV panel selection while ensuring system reliability. The proposed system was optimized using improved Differential Evolution (DE) and its effectiveness was tested by comparing the results with Particle Swarm Optimization (PSO) and Genetic Algorithm (GA). The Improved DE algorithm provides the highest average cost savings compared to other algorithms, which is $500 per year. It is recommended that this method is very useful in the optimization of off-grid PV systems, considering other uncertainties that affect PV system performance.

Keywords: Off-Grid flow, Optimization, Photovoltaic, Battery, Levelized cost of Energy

Abstrak

Penghasilan kuasa secara konvensional adalah salah satu penyumbang kepada kesan kumah hijau. Perkara ini mendorong ke arah kepelbagaian sumber tenaga termasuk tenaga mesra alam seperti tenaga solar. Sistem solar terasing telah menarik minat disebabkan kos berpatutan untuk kawasan pedalaman. Walaubagaimanapun, tenga solar yang tidak tetap manjadi cabaran utama dalam membangunkan system solar terasing. Tambahan, kos pembangunan PV dan bateri penyimpan menjadi kebimbangan utama kepada pengguna PV. Oleh itu, tujuan utama penyelidikan ini adalah untuk menentukan saiz PV dan bateri secara serentak dan merekabentuk sistem PV yang kos efektif dengan mengambil kira pelbagai aspek seperti kuasa bateri, solar radiasi dan pemilihan PV

panel. Dan dalam pada masa yang sama memastikan kebolehpercayaan sistem terjamin. Sistem yang direkabentuk kemudiannya di uji menggunakan DE yang telah ditambahbaik dan kemudiannya keberkesanannya dibandingkan dengan PSO dan GA. DE yang telah dikemaskini memberi purata penjimatan kost yang tertinggi berbanding dengan algorithm lain iaitu $500 setiap tahun. Ini menunjukkan kaedah ini sangat berguna dalam mencari sistem yang optimum.

Kata kunci: Pengaliran PV terasing, pengoptimuman, fotovaltaik, bateri, kos PV yang disekatakan

1.0 INTRODUCTION

The continuous depletion of fossil fuel sources and the drive to combat carbon dioxide (CO_2) emissions have led to the exploration of renewable energy sources [1,2]. In 2018, the transition to renewable energy like solar, wind, and biomass in the power sector had a positive impact on CO_2 emissions, as 215 Mt of emissions were reduced [2]. This is due to a 7% increment in electricity generation from sustainable sources that added 450 TWh to global power generation [2]. Without this transition, global CO_2 emissions could have reached 1.5 Gt, an increase of 11% in emissions from the current power sector [2].

In this context, it is crucial to use energy that is sustainable, economical, and less risky for the environment, while meeting the increasing energy demand [3]. The photovoltaic (PV) system can be considered the most far-reaching solution that is at the cutting edge of progress while guaranteeing the energy era with low environmental impact [4]. PV technology is quiet and clean, as it works with the radiation emitted by the sun, unlike traditional fossil fuels [3]. In addition, the installation of PV systems does not occupy a large space because the small solar-powered systems can utilize unused areas on rooftops of existing buildings. Installing PV systems in rural communities in African countries is practical due to ineffective conventional infrastructure to supply electricity where it is far from the national grid or transmission infrastructure [5]. The poor nature of the road network connecting these distant communities makes it impossible to install generators and transport fuel to generate electricity in such an environment. The amount of solar radiation and the duration of solar radiation in most African countries make the use of the sun the most important source of energy in the future [6].

Over the years, this has brought into focus the discussion on inexhaustible, sustainable, and environmentally sound energy. Several research areas are aimed at developing off-grid PV systems that will be integrated into the architecture of the power grid of buildings, not only to solve the problem of electricity generation but also to provide a source of income for the owners of the buildings [7]. This development study includes a comparative study by Kamran *et al.* that investigated three hybrid systems consisting of diesel generators, hydropower, PV, and battery in rural Punjab, Pakistan [8]. HOMER was used in the economic analysis to determine which offers the better net profit cost (NPC) for energy per kilowatt among the three designs, based on BS link canal-1. The optimization result shows that the hydro and solar storage system offers an optimal solution with better NPC [8].

In the electrification of rural residential houses in Cyprus, a mathematical model was used to determine the different parameters of the systems in the feasibility analysis of an island PV system conducted by Kamali, S. [9]. The life cycle cost, annualized life cycle cost including the unit price of electricity was determined[9]. However, the authors do not address the basic strategy for the off-grid configuration. The ideal configuration of the electrical power supply system is discovered in [10] using linear programming techniques in the General Algebraic Modeling System (GAMS) environment, taking into account characteristic constraints as well as hourly weather data, demand data, the tilt angle of PV models and shades analysis.

The research carried out in [11] focuses on the optimization of an off-grid hybrid PV-wind-diesel system with different battery technologies is performed using a Genetic Algorithm (GA). The optimization considered the PV system sizing, mechanical structure, battery, inverter, charge controller, and tilt angle. However, only uncertainties of solar radiation are considered in the study. Eteiba *et al.* proposed a hybrid system with an economic analysis based on Harmony Search (HS), Flower Pollination (FPA), Artificial Bee Colony (ABC), and Firefly Algorithm (FA)[12]. The aim was to find the most suitable algorithm to achieve optimal sizing of the hybrid system. The result showed that FA is the fastest way to achieve the optimal solution, followed by HS and FPA, while ABC needs more time to accomplish the same outcome [12]. Islam *et al.* [13] carried out a comparative study to observe the performance of GA, Particle Swarm Optimization (PSO), and Differential Evolution (DE) in smart grid optimization problems. The result shows that employing DE algorithm can significantly minimize the problem with less computational time [13].

In a comparative study conducted by Ouyang & Pano, [14] three metaheuristic algorithms DE, GA, and PSO were used to optimize the gain of PID controller for tuning and performance evaluation. DE algorithm performed better than GA and PSO for both linear and nonlinear contours. This was attributed to the

competence in population diversity and the mutation process, which makes DE more adaptive in staying away from local minima. To improve the performance of DE, *Gao et al*. [15] introduced a directional permutation differential evolution algorithm (DPDE) to determine the optimal solar PV parameters. The performance of the proposed algorithm is compared with the other 15 algorithms. The results show that DPDE performs better than its competitors in terms of solution accuracy.

The DE algorithm is known for its better global convergence and robustness, and is suitable for a wide range of optimization problems, quickly making it an ideal algorithm in current optimization domains [16]. In DE, the population consists of several individuals, each of which represents a possible solution to an optimization problem. DE generates individual offspring through mutation, crossover, and selection, which must converge to the ideal solution. Implementation of mutation to all competitors characterizes an investigation rule on other candidate solutions. Regardless of the capability of DE, some adjustments are basic fundamental to improve its performance, particularly in tending to high-dimension issues [17]. Stagnation, untimely combination and its sensitivity to control parameters such as tuning of PVs and batteries are some of the problems that impact the exhibition of DE [18].

To address these shortcomings of DE, numerous improvements were proposed, most of which focused on control parameters and mutation techniques. Population size NP, scaling factor F, and crossover CR are three key control parameters. In many works in the literature, there is evidence that the performance of DE can be improved by changing these control parameters [19].

Hybridization of DE with other evolutionary algorithms has led to remarkable optimization results due to its flexibility in interaction with other algorithms [20]. Based on the literature in optimization area over the years show that the use of batteries in conjunction with renewable energy is reliable and environmentally friendly [3].

However, several optimization problems are not direct and unexplored [21] such as uncertainties related to renewable energy sources, load demand, and non-linear characteristics of certain parts [4]. Moreover, the high capital cost of PV systems and storage batteries compared to conventional fossil fuel power plants is a major obstacle affecting their deployment on a larger scale. However, this factor is less considered in existing research. Considering the above studies, this study aims to design a cost-effective off-grid PV system that takes into account various aspects such as battery power, solar irradiance, and PV panel selection, while ensuring the reliability of the system. The size of the PV system and the battery are optimized simultaneously using the improved DE. The improved DE is introduced by adopting the iteration-dependent factor (λ) in the mutation process. This proposed method provides better exploration and exploitation in the optimization process.

2.0 MODELLING OF OFF-GRID PV SYSTEM

The modelling process focuses on optimizing the PV and battery size using the improved DE algorithm. The optimization process starts by randomizing the number of PV and battery sizes simultaneously as shown in the flow chart of Figure 1. The irradiance level is then called to access the level of energy that can be harnessed from the irradiance. The hourly solar irradiance data that are obtained from NASA are utilized.

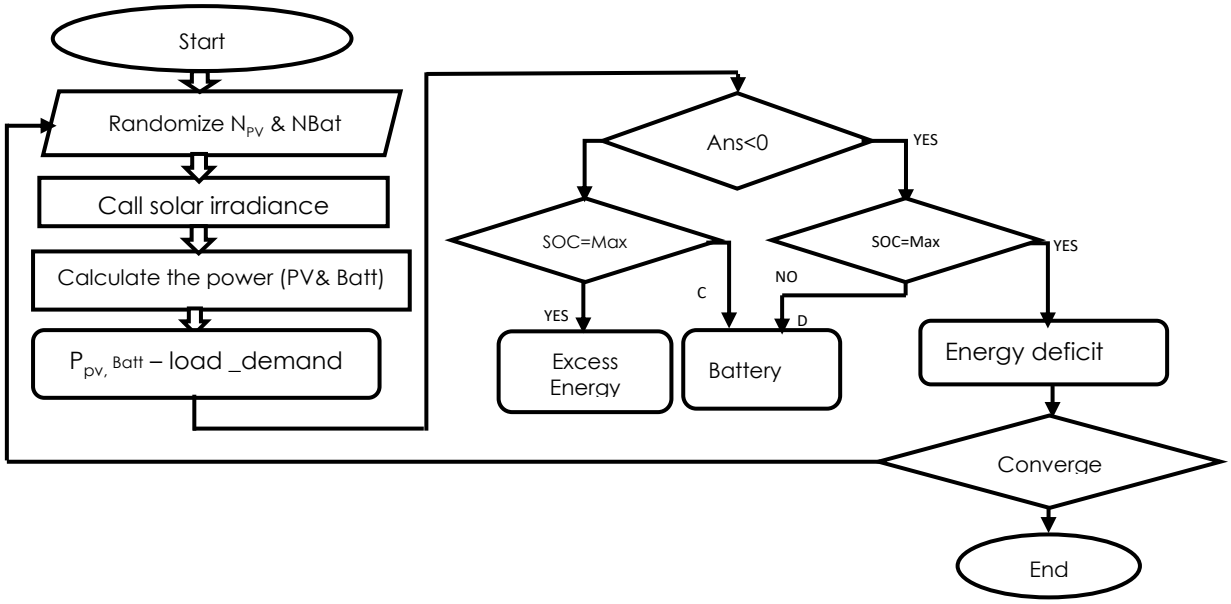

Figure 1 Flow chart for the optimization process

Based on the randomized PV number and solar irradiance, the power produced by the PV, P_{PV} and power stored in the battery are determined. The net power of PV and battery, P_{PVBatt} is then calculated and matches the load demand. At the point where there is excess solar energy available, the excess energy from the PV is stored in the battery storage until it is completely charged. On the other hand, the battery will be released and constrained by a charge controller to supply the load if solar PV is deficient or inexistent to avoid the battery's fast degrading which will affect its lifetime.

Typically, an off-grid PV system comprises four fundamental segments, which are the PV module, battery storage, charge controller and inverter. The power supplied by the PV system feeds both the load and the storage battery being regulated by the charge controller. The excess energy from the PV that circulates in the system is stored by the battery storage until it is completely charged. On the other hand, the battery is released to supply the load when the solar energy is deficient and also to ensure the two constraints, SOC and load demand requirement are met.

2.1 PV Array Modelling

The output energy obtained from the PV is calculated based on the peak sun hours and ambient temperature [22]. Loss of efficiency due to high-temperature F_{loss} (t) and energy generated by PV (P_{sol}(t) are respectively estimated in equation (1) and (2).

$$F_{loss}(t) = (1-(T(t)-25\times\beta_{ref}) \quad (1)$$

Where T(t) must be greater than 25°C.

$$P_{sol}(t) = F_{loss}(t)\times \Pr\times\frac{Gh(t)}{GS} \quad (2)$$

where, βref the temperature coefficient, ($P_{sol}(t)$ is the output power of a single solar panel and Pr manufacturer's power rating of a single PV. GS is the standard incidence radiation (1000 W/m^2) while $Gh(t)$ is the series irradiance data recorded at the location. In this study, the 0.0038K is chosen for βref [23] and 315W SPR-315E-WHT-D monocrystalline cell is selected as a PV model.

Traditional method can also be adopted in implementing PV systems. In this approach the number of PV panels required for a specific installation is given by,

$$N_{PV} = \frac{(E_{req-Daily}/(H_{Oa}\times\eta_S))}{P_{PV}} \quad (3)$$

Where N_{PV} is the Number of PVs, $E_{req-Daily}$ daily energy consumption in watt-hours, H_{oa} average daily solar radiation, η_s system efficiency and P_{PV} is the PV panel power rating. The module efficiency, inverter efficiency, wiring efficiency, and other system losses constitute the system efficiency. The average solar radiation received by Ghana each day ranges from 4.0 to 6.5 kWh/m^2, with sunlight hours per year averaging 1800 to 3000h [24].

The traditional method of estimating the number of PVs and batteries for a solar power system involves determining the daily energy needs, calculating the daily solar energy production, sizing the PV and battery systems, and adding safety and redundancy factors.

The location chosen for this study is located in the southern part of Ghana where the rainfall pattern is enormous during the rainy seasons. Therefore, replicating this in a similar or better geographical location will result in optimal-size PVs and storage battery systems.

2.2 Irradiance Data Modelling

Solar radiation modelling is carried out by studying the solar orbit and its effect on the solar panels and how much energy can be generated [25]. In this model, the parametric component to be considered is the time and day of the year. The maximum amount of incident solar radiation is measured on an inclined surface, whereas global solar radiation is typically measured on a flat surface [26]. Global solar radiation is typically measured on horizontal surfaces at weather stations. However, most stationary solar systems, including solar photovoltaic and flat plate solar collectors, are positioned on inclined surfaces to fully exploit the sun radiation on collector surfaces.

Finding the best accurate model for each region is necessary due to the latitude that has a significant impact on estimating models. Comparing measured values and estimated values using various statistical indicators will reveal an accurate model [24, 25]. The boundary parameters are utilized in determining the sun's elevation, declination, and azimuth, the tilt angle of the earth pivot, and the tilt angle of PV cells [28].

2.3 Temperature Modelling

The output voltage of a PV model is affected by temperature variations. The output voltage is highly dependent on temperature and an increase in temperature leads to a decrease in output voltage[29]. The widely used method to model the temperature of a PV cell is by utilizing the nominal operating temperature (NOCT) of the PV module concerning the Ross model that is expressed in Equation (4).

$$T_C = T_a + \frac{(T_{NOCT}-20)}{800}\times Gh(t) \quad (4)$$

where T_C is the temperature of the PV cell, T_a is the ambient temperature, $Gh(t)$ is the series irradiance data, and T_{NOCT} is the Nominal Operating Cell Temperature. The NOCT of 315W SPR-315E-WHT-D cell of 46.0°C was used.

2.4 Load Modelling

Load profile characteristics are an essential component in determining the reliability and appropriate sizing of an off-grid system. Proper modelling of the load profile provides a reliable load forecast of how much energy is needed to power the off-grid PV systems. The load profile is modelled in this study based on residential energy demand assessment data obtained from the Ghana Power Utility company.

2.5 Battery Storage Modelling

The state of charge SOC of the battery at any time *t* (hour), is identified with the preceding SOC [SOC(*t*–1)] that relates to the production of energy and utilization circumstance of the system within a duration of (*t*-1 to *t*) [30]. In this charging process, when the battery power P_{Batt} (*t*) at time *t* flow towards the battery (i.e., P_{Batt} (*t*) > 0), the accessible battery SOC at time *t* (hour) can be estimated by equation (5).

$$SOC_{(t)} = SOC(t-1) + \frac{P_{Batt} \times \Delta t}{1000 \times C_{\_rated}} \quad (5)$$

where $C_{\_rated}$ is the nominal total capacity of a battery in kilowatt-hours and Δt is the step time of simulation (set equal to 1hr). Furthermore, when the battery is discharging, the battery power flows outside of them (i.e., P_B<0), so the accessible battery charge at time *t* can be expressed using equation (6).

$$SOC_{(t)} = SOC(t-1) - \frac{P_{Batt} \times \Delta t}{1000 \times C_{\_rated}} \quad (6)$$

The discharge capacity ($C_{\_discharge}$) of a working battery is the discharge energy limit when it is discharged. Likewise, the SOC is characterized as the percentage level of discharge limit compared with the battery-rated capacity ($C_{\_rated}$), as a state by the manufacturer [31].

$$SOC = \frac{C\_discharge}{C\_rated} \times 100 \quad (7)$$

Disregarding the effect of ageing and the operational efficiency of the battery, the SOC is calculated using equation (8).

$$SOC(t) = 100\% - DOD(t) \quad (8)$$

To ensure that the battery life is prolonged, the battery ought not to be overcharged or discharged. This implies that SOC at any hour *t* should conform to the set constraints.

$$(1 - DOD_{\max}) \le SOC(t) \le SOC_{\max} \quad (9)$$

where DOD_{max} and SOC_{max} are the maximum allowable depth of discharge and state of charge respectively. The storage capacity of the battery required (C_{bank_req}) during the days of autonomy and the rate of discharge of energy from the battery is determined by the Depth of Discharge (DoD) [32]. The greater the DoD and temperature adjustment factor *(Mf_{tem_Batt})* of a battery, the better the output that depends on the battery manufacturer's temperature characteristics [33] [34]. The required charge daily, (C_{req_daily}) and the required battery bank capacity (C_{bank_req}) is determined by equation (10) and (11) respectively. This formular also consider 85% efficiency factor that accounts for energy losses due to battery charging and discharging.

$$C_{req\_daily} = \frac{E_{req\_Daily}}{SV} \times \frac{T\_autonomy}{DoD_{\max}} \quad (10)$$

where SV is the system voltage as a state by the manufacturer on the nameplate in the order of 6,12V, 24V, or 48V, etc. To determine the capacity of the battery bank required (C_{bank_req}) the daily charge required (C_{req_daily}) is substituted given Equation (11).

$$C_{bank\_req} = C_{req\_daily} \times \frac{T\_autonomy}{DoD_{\max} \times Mf_{temp\_Batt}} \quad (11)$$

where Mf_{temp_Batt} is the temperature derating factor of the battery. The charge required is given by the Output of the PV array (Ah) and must be greater than $C_{required\_daily}$. $T_{\_autonomy}$ is the coefficient that determines the period within which the battery is capable of meeting the load demand without any energy from the PV which is normally taken as 4 days [35]. It is essential to design the Off-Grid PV system with a maximum daily SOC of less than 20% in other to prolong the life span of the battery. In determining the daily SOC, equation (12) is used.

$$DoD_{\_daily} = \frac{C_{req\_daily}}{C_{bank\_selected}} \quad (12)$$

2.6 Problem Formulation

The variables to be optimized are the number of PVs and batteries. The objective of the formulated problem is to minimize the initial cost of PV and the battery including the inverter as in equations (13), (14), (15) and (16) [33].

$$f = Min(C_{PV} + C_{Batt} + C_{inv}) \quad (13)$$

$$C_{Batt} = \frac{[N_{batt} * (1 + Batt\_C * (i * (1+i).\wedge (Bat\_L)]}{[(1+i).\wedge Bat\_L) - 1)]} \quad (14)$$

$$C_{PV} = \frac{[N_{sol} * (P_{PV}/GS) + C_{sol} * (i * (1+i).\wedge (PV\_L)]}{[(1+i).\wedge PV\_L) - 1)]} \quad (15)$$

$$C_{inv} = \frac{[N_{sol} * (1 + inv\_C * (i * (1+i).\wedge (Bat\_L)]}{[(1+i).\wedge Bat\_L) - 1)] * (P_{PV}/GS)]} \quad (16)$$

Where C_{Batt} is the cost of the battery, C_{PV}, is the cost of PV, C_{inv} is the cost of the inverter, N_{sol} is the number of solar panels, PV_L is PV lifetime, P_{PV} is the power rating of the selected PV, N_{batt} the number of batteries $Batt\_C$ the unit cost of the battery, Bat_L lifetime and *Csol* is the unit cost of the solar panel.

The constraints play a significant role in the formulating of algorithms and programming for the general obliged issue. Thus, the related cost is minimized while satisfying battery constraints. The SOC must be greater than 21% [35] and the PV output must be greater than the charge required. In addition, the load demand should be met by either PV or battery, which means that at each instant sufficient power should be available.

The economic cost analysis is an integral part of evaluating the returns of an Off-Grid PV system. One of the economic analysis tools is the Levelized Cost of Energy (LOCE) whereby the life cycle cost of the off-grid system is estimated using equations (17) and (18) [36].

$$[Annual_{C_{PV}, C_{Batt}, C_{inv}}] = economic\_cost(x(2), x(1), 0) \quad (17)$$

$$LCOE = Annual\_cost / sum(load1) / 3 \quad (18)$$

Where load1 is the estimated load at the location for the period under study.

3.0 OPTIMIZATION OF OFF-GRID PV SYSTEM USING IMPROVED DE ALGORITHM

The off-grid PV system is optimized using an improved DE algorithm. The effectiveness of the proposed algorithm is observed by comparing it with GA and PSO. Since the number of variables to be optimized is two which are the number of PV systems and batteries, the population size (NP) is set to 20 where the recommended population size is ten times the problem dimension [37]. A mutation factor of 0.5 and a crossover rate of 0.7 were chosen. Details of the solar modules, battery units, and inverters considered are given in Table 2. The algorithm uses the standard test conditions (STC) of a 315W SPR-315E-WHT-D monocrystalline cell with a nominal cell temperature (NOCT) of 46.0°C to determine the optimal photovoltaic (PV) system size [38] and selects 1400 battery units as the upper boundary that have sufficient ampere-hour (Ah) capacity to meet the load demand of the autonomy days. 1000 and 1400 were set as the upper limit of the search space for the PV unit and the battery unit, respectively, while 1 was set as the lower limit of the search space for the PV unit and the battery unit.

3.1 Improved Differential Evolution Algorithm

The improved DE algorithm searches for the optimum global point i a D-dimensional real parameter of a given space [39]. The initialization starts with a randomly initiated populace of NP D dimensional genuine esteemed parameter vectors. Like other developmental strategies, DE manages a populace, G^i, of candidate solutions [40]. The populace contains NP solutions. Every solution X_n^i contains a lot of the optimizing parameters x_n. The lower optimum limit of PV modules and battery units are set to unity, which implies that at least one PV module and one battery unit are chosen. This limit is the lowest possible practical limit. The maximum number of battery units that can be selected by the DE is limited by the load demand during the days of autonomy [41].

$$G^i = [X_1, X_2, X_3, , , X_{NP}]^T \tag{19}$$

$$X_n{}^i = [x_{n1,} x_{n2,} x_{n3,,,,} x_{nD,}] \tag{20}$$

3.2 Initialization

DE begins with the underlying populace produced randomly utilizing the lower and upper limits as shown in equation (22).

$$x_{ij} = x_{j,\min} + Rand * (x_{j,\max} - x_{j,\min}) \tag{21}$$

$$i = 1,2...., NP and j = 1,2...D \tag{22}$$

where G_{max} is the maximum number of generations, NP is the population size, D is the number of parameters to be optimized, $x_{j,min}$ is the lower bound of optimized parameter j, $x_{j,max}$ is the upper bound of optimized parameter j.

3.3 Improved Mutation Process

The mutation process takes part after the initialization. This process is the primary segment that distinguishes DE from other populace algorithms [17]. Applying the mutation to all competitors characterizes an investigation rule depending on other candidate solutions. Regardless of the capability of DE, it is clear to researchers that some adjustment to DE is a basic fundamental to improve its performance, particularly for high-dimensional issues [17]. Stagnation, untimely combination, and its sensitivity to control parameters such as tuning of PVs and batteries are some of the principles that affect the exhibition of DE. DE is exceptionally reliant on the control parameters involved [42, 43]. Fine-tuning these fundamental parameters in practice is very cumbersome depending on the complexity of the problem. However, improving the mutation of the DE Algorithm will keep the multiplicity of the population and also enhance the capacity of the local search [43] with less computational time to achieve a desirable solution.

The mutation activity is appraised as the initial move toward the age of a new solution [44]. Then, for each solution in the population, $X_i{}^{(t)}$ two solutions $X_{r1}{}^{(t)}, X_{r2}{}^{(t)}$ are randomly chosen and a freak vector $V_i{}^{(G)}$ is created as shown in equation (23) [45].

$$V_i(g+1) = X_{r1}(g) + F.(X_{r2}(g) - X_{r3}(g)) \tag{23}$$

where $i \neq r_1 \neq r_2 = r_3, i = 1,2...NP$ are randomized integers generated from the set, g the current iteration number of the generation, and a new population is generated as $V_i(g+1)$ i.e., the quantity of the optimized parameters [46].

$$DE/rand/1 \rightarrow V_i^t = x^t_{r1} + F(x^t_{r2} - x^t_{r3}) \tag{24}$$

$$j = 1,2,..,...D$$

$$DE/best/1 \rightarrow V_i^t = x^t_{best} + F(x^t_{r2} - x^t_{r3}) \tag{25}$$

Considering equations (24) and (25), $x^t_{r1,} x^t_{r2,} x^t_{r3}$ are different randomized individuals that are not the same as one another. Meanwhile, x^t_{best} is the best individual in the populace. F is the mutation factor which is set within [0, 1] [45, 49].

Consolidating the attributes of these two diverse mutation strategies, the impacts of random individuals $X^t{}_{r3,}$ and ideal individuals $X^t{}_{best,}$ are taken into account when making the transformation process of the mutation equation [46] [47]. Thus, the mutation strategy adopted is written in equations (26) and (27).

$$V_i^t = \lambda x^t_{r1} + (1-\lambda) x^t_{best} + F(x^t_{r2} - x^t_{r3}) \tag{26}$$

$$\lambda = (T_{\_\max} - t)/T_{\_\max} \tag{27}$$

where λϵ [0, 1]. If λ= 1 then equation (26) turns into equation (24). Meanwhile, equation (27) turns into

equation (25) that corresponds with *DE/rand/1* and *DE/best/1* respectively if λ=0. T_max is the largest number of iterations and t is the current number of iterations. Thus in the evolutionary process, λ can gradually change from 1 to 0 to realize combining local search with global search [46]. Accordingly, λ is set as the annealing factor as shown in equation (27). Integrating the local and the global search capabilities offers the best precision and convergence rate thereby improving the mutation process [46].

3.4 Constraint

Loss of load probability (LoLP) is a statistical parameter that portrays the chances of failure in power supply either due to low resource availability to meet energy demand or due to technical failure. LoLP is calculated using equation (27).

$$LoLP = \frac{\Sigma (P_{Load}(t) - P_{pv\_out}(t) + P_B(t))}{\Sigma P_{Load}(t)} \quad (28)$$

3.5 Finding the Optimal Solution

To find the global, or near-global, optimal solution, the candidate solution objective function estimation is compared with that of the best solution objective in the following generation [40].

4.0 RESULTS AND DISCUSSION

The allocation of an Off-Grid PV system for households for a small community located in Ghana at longitude and latitude coordinates of -1◦35'59.99 and 5◦54'59.99, respectively. Annual solar irradiance data of the site is shown in Figure 2 were taken from the NASA website. Considering the radiation pattern, it is evident that the location has the potential to implement the Off-grid PV system.

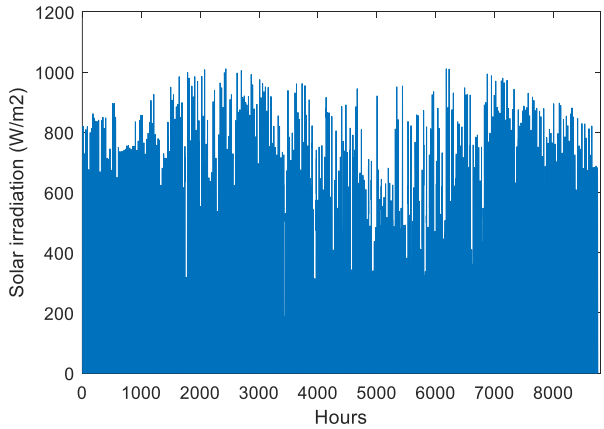

Figure 2 Annual Solar irradiation of location

Nevertheless, the proper implementation of an Off-grid PV system is highly important to maximize the benefit of the solar energy system. Furthermore, the installation of solar panels at a proper elevation of tilt angle contributes significantly to maximizing the output power of the generation.

The optimum tilt angle is analyzed by adding 15° to the latitude in the winter and subtracting 15° from the latitude during the summer. Since the site under study is located -1.355˚ North and 5.545˚ West longitude, therefore the solar panels' optimal angle is adjusted to be 15˚ facing southward. For fixed and non-rotational panel systems, the aforementioned tilt angles were chosen for the optimal year [3]. Testing of photovoltaic modules is carried out at a temperature of 25°C (STC) which is about 77 degrees on the Fahrenheit (F) scale. Depending on the location of the installation, the temperature can affect the efficiency of the output by 10-25% [48].

This results in an exponential increase in current and a linear decrease in voltage [23]. Figure 3 shows the temperature of the location ranging from 19-38 °C. The result shows that the maximum temperature is 38°C. The cell temperature is determined by steady-state power balance. An assumption is commonly made that states that a drop in cell-ambient temperature increases linearly with irradiance [23].

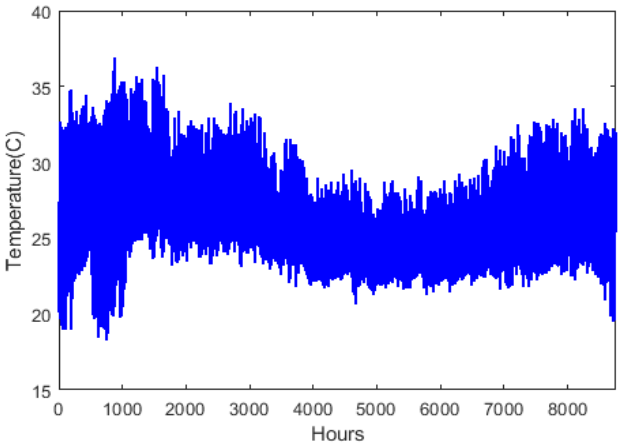

Figure 3 Annual temperature location

4.1 Sizing of Off-grid PV System

Sizing of PV and battery are conducted based on the manufacturer's datasheet of the selected PV panel, type of battery storage, Inverter type and the economic rate of interest, and other factors as provided in Table 1.

Table 1 Technical specification and economics of the system

Type	315W SPR-315E-WHT-D MONOCRYSTALLINE CELL	SI UNITs
	STC Power Rating Pmp (W)	315 W
	Open Circuit Voltage Voc (V)	64.6 V
	Short Circuit Current Isc (A)	6.14 A
	Nominal Operating Cell Temperature (NOCT)	46.0°C
	Panel Efficiency	19.3%
	Fill Factor	79.4%
	Unit Price (USD)	416.078
	Life expectancy	25 years
Deep-Cycle Flooded/Wet Lead-Acid Battery		

Type	315W SPR-315E-WHT-D MONOCRYSTALLINE CELL	SI UNITs
	Trojan J305H-AC Flooded Battery	360Ah
	System Voltage	6.0V
	Bulk Charge	7.14V
	Unit Price (USD)	408.66
	Life expectancy	5years
	Operating Temperature:	-20+55°C
APOLLO STP-2110 Cp (L) Bidirectional Parallel Inverter		
	At 25.0 °C. CosΦ= 1	18KVA
	Nominal Voltage	48 VDC
	Maximum charging current	240 A
	Efficiency	95%
	Economic parameters	
	Interest rate	6%
	Inflation rate	1%
	Operation and maintenance cost	usd1/KW

This includes the power ratings, efficiencies NOCT of the PV cell, and the operating temperature of the battery. The load demand is supplied by solar energy and battery bank. In the daytime when sufficient solar energy is available, the load is supplied by the solar panel, while in the days of autonomy period battery storage is used to supply the required energy. To maintain a continuous balance between electricity production and consumption, there are strict constraints on the whole system.

It is important to have in full sight the 24-hour load profile which best analyses the consumption pattern to determine the appropriate sizing for PV and battery. A typical 24-hour load profile of a residential housing unit is shown in Figure 4 with the maximum load demand recorded in the evening hour of the day. This is normal because consumers leave their various homes in the daytime to their farms and place of work and return home in the late afternoon resulting in a load rise that continues to the evening.

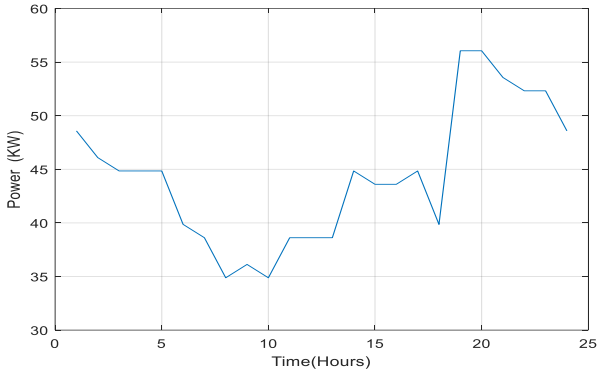

Figure 4 24 hours load profile of location

The efficiency of the photovoltaic panel, battery, and inverter as provided by the manufacturer's datasheet are 19.3%, 90%, and 95%, respectively. Furthermore, the highest maximum load demand of the system recorded is 57 kW as shown in Figure 4. The load is expected to remain within this range looking at the load pattern.

4.2 Optimization Algorithms Results

The improved DE algorithm optimizes the size of the PV and battery to reduce the overall cost of the system based on two constraints and boundary conditions. The annual cost of the system's energy production was chosen as the objective function. The system analyzed three years of data and the results are based on the best fitness function. The results of the improved DE algorithm converged in less than 50 iterations. The optimization of DE results in an optimal number of 1154 PV units with 315 W solar-powered monocrystalline cells and 813 battery units of 360Ah each. This means that the peak power of the PV source is 363.5 KW. The result for the optimal sizing of the off-grid PV system with the battery using DE, PSO, and GA is shown in Table 2. The result shows a significant reduction in the electricity price with improved DE compared to PSO and GA. For the electricity cost (USD/kWh), by reducing the proportion of PV system and battery, some useful results are obtained, which lead to significant savings in annual energy cost and electricity cost.

Table 2 Optimum Sizing using improved DE, PSO and GA

Description	DE	PSO	GA
No. of PV modules	1154.0	1161.0	1170.0
No. of Battery units	823.0	824.0	825.0
Load served (kWh)	351.49	351.49	351.49
Annual cost of energy (USD)	73438.0	73946	73949
Cost of energy per kwh	0.2089	0.2104	0.2104
Function count	243.86	1960	3841
Number of Iterations	50	97	95
Constraints Violated	13759	13735	1780

The function count shown in Table 2 indicates how many times the algorithm is executed depending on the loop used in the program. The loop defines the time complexity of the program, and is always prudent to reduce the loops in a program thereby reducing time complexity.

In accessing the performance of the system, the response time is of great essence. The function count of the various algorithm is a determinant factor in ensuring faster convergence. One of the simplest ways to handle constraints is through the penalty function method. It operates by punishing the impractical candidate solutions and changing the confined optimization problems into their unconstrained equivalents [49]. By creating a fictitious penalty for breaking the constraint, penalty functions aim to transform constrained issues into unconstrained problems.

Equations (3) and (10) were used to compare the simulated optimized result to the traditional method, based on the system specifications in Table 1 and the estimated load demand of 351.49kWh in Table 2. The number of PVs (NPV) obtained from equation 3 is 1213 PV modules, whereas the DE simulated result in table 2 yields 1154 PV modules. The size of the battery bank is determined by the amount of energy to be stored and the maximum DoD recommended for the battery type. Using equation (10) and the Trojan J305H-AC Flooded Battery's autonomy day of 4, DOD of 80%, efficiency factor of 85% due to battery charging and discharging, and 360Ah rating as shown in Table1. The traditional

method required 958 batteries, whereas the DE required 823 batteries, as shown in Table 2. The results show that the number of PVs and batteries obtained using the traditional method far outnumber those obtained using the three algorithms. Overengineering a PV system leads to decreased energy efficiency and significant financial losses, such as higher upfront costs and higher maintenance costs.

4.3 State of Charge of Battery Bank

The charging and discharging characteristics of the battery bank for one week on an hourly basis are shown in Figures 5 and 6. It can be seen that the state of charge of the battery is slightly higher than the load demand, which ensures the reliability of the system. It can also be seen that the energy generated is far sufficient to meet both the load demand and the storage bank.

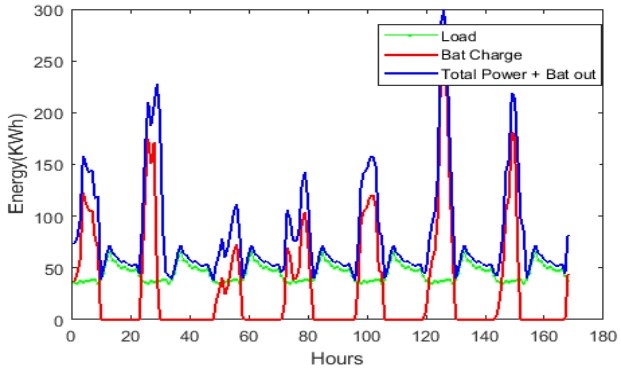

Figure 5 Hourly PV generation, battery and load profile

The weekly SOC in Figure 6 shows the uncertainties of irradiance and its impact on PV system performance. This plays a critical role in determining the objective function and its implication on cost analysis concerning the storage requirements of the system. Analysis of 20 years of solar irradiance historical data is modelled to mitigate these uncertainties.

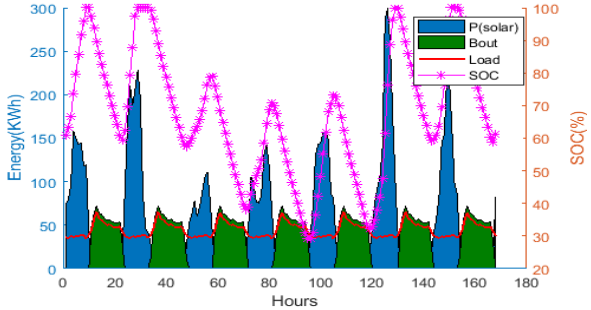

Figure 6 A week plot of load, irradiance, battery and SOC

Optimally selecting storage capacity is to ensure that the cost of the system is reduced since storage batteries and PV panels constitute 65% of the entire cost of installing PVs [50].

In this study four days autonomy period is considered effective in addressing the constraint of prolonged non-sunny days. To evaluate the electrical performance among the three algorithms the same number of PVs and batteries 1154, 823 respectively was used to run the PSO, DE and GA algorithms. The result in Figure 7 below shows the outcome of three algorithms showing clearly that the PSO and GA have violated the constraint of the SoC of 80% set for the successful operation of the system. This means the battery will discharge beyond 80% allowable limit which when allowed will affect the performance of the battery, especially the cycle life.

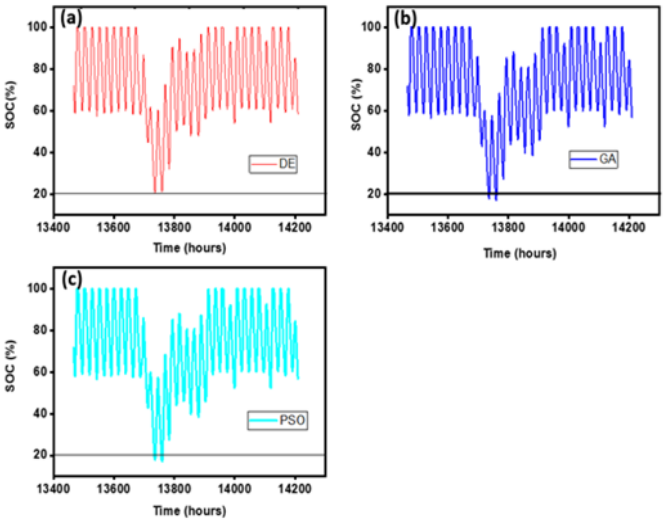

Figure 7 Optimised SOC for (a) DE (b) PSO and (c) GA plotted

The battery capacity available for a cell is indicated by its state of charge (SOC), which is a function of its rated capacity. The SOC value ranges from zero to one hundred per cent. The cell is said to be fully charged if the SOC is 100 per cent, while an SOC of 0 per cent denotes a discharged cell. Thus, the restricted depth of discharge was set at 0.8, implying that the battery bank can discharge 80% of its charged capacity with a reserve margin of 20%.

The SOC of DE shown in Figure 7 indicates that the battery bank has sufficient capacity to meet the load demand during the days of autonomy.

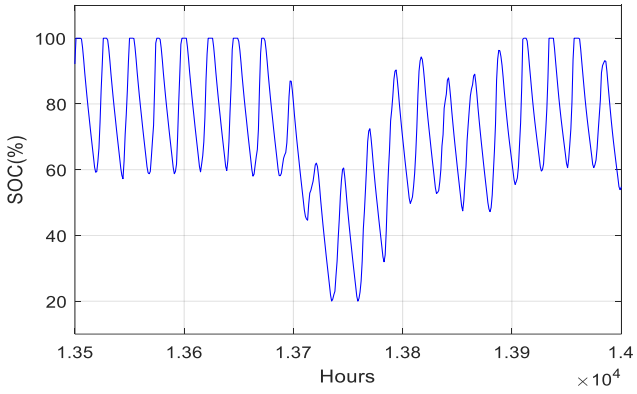

Figure 8 SOC of the battery for the worst month

To ensure that the system is optimally selected and the PV modules and battery units are not overly designed, the lower PV modules than the optimized size are tested. According to Figure 8, the SOC

measured between 13700 and 13800 hours was the worst, dropping to the 20% constrained value. The State of Charge (SOC) of a battery reaches a specified minimum SOC threshold when it reaches a limited value of 20%, which is set by the system or application. This restriction is put in place to guarantee that the battery is kept at a minimum level of charge for a variety of reasons, including safety, performance, or longevity. Figure 9 is an SOC performance when the 1130 PV modules are applied. The result shows that when the number of PV modules are reduced, the SOC of the battery bank decreases below the threshold value, violating the constraint, so the selected design is optimal. The reduction of the number of PVs results in worse SOC performance.

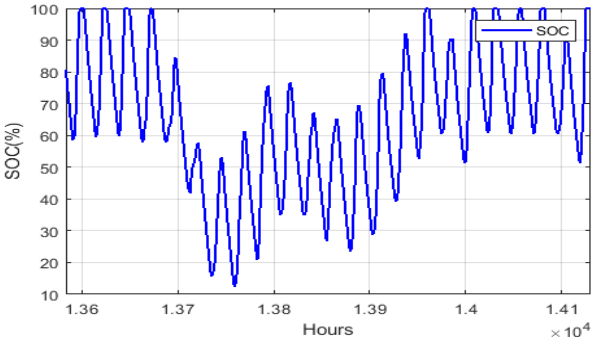

Figure 9 System SOC with reduced PV below optimal design

4.3 Economic Cost Analysis

The Levelized Cost of energy is dependent on the efficiency of the battery bank and converter efficiency. The Levelized cost of electricity (LCOE) increases when either the battery bank or the efficiency of the converter decreased. When the converter efficiency decreases, a lot of energy is lost from the battery bank during conversion, resulting in the need for a large battery bank. Consequently, it increases the cost of energy per kilowatt.

By implementing the improved DE algorithm to the optimization problem, the detailed analysis of the LCOE with change in efficiency is presented in Figure10 below while the cost of energy per kWh is shown in Figure 11. The cost of energy per kWh from the result among the three optimization methods (improved DE, PSO, and GA) adopted stood at 0.2089, 0.2104, and 0.2104 USD, respectively as shown in Table 2. An average annual cost savings of 500 USD is obtained by the improved DE algorithm when compared with the PSO and GA algorithms.

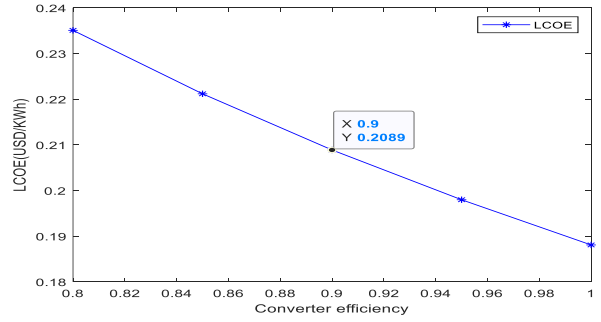

Figure 10 Variation of LCOE with change in converter efficiency

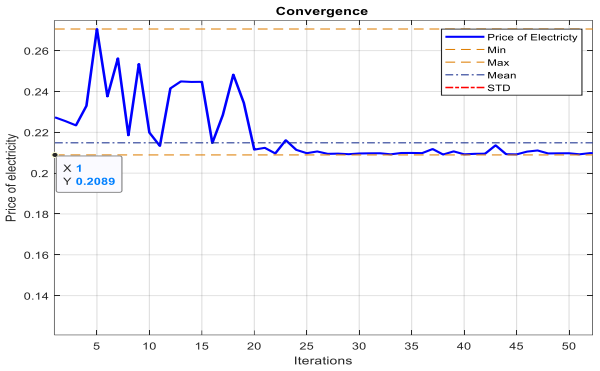

Figure 11 Variation of iteration vs price of electricity for DE

In each case, the simulation of the optimization algorithm is performed for three different values of loss of power supply probability (0%, 0.1%, and 0.6%).

Figures 11, 12, 13 and 14 present the evaluation of the price of energy obtained using the DE, PSO and GA, respectively for Loss of Load Probability (LOLP). These results validate further the overall superiority of the improved DE performances compared to the PSO and GA.

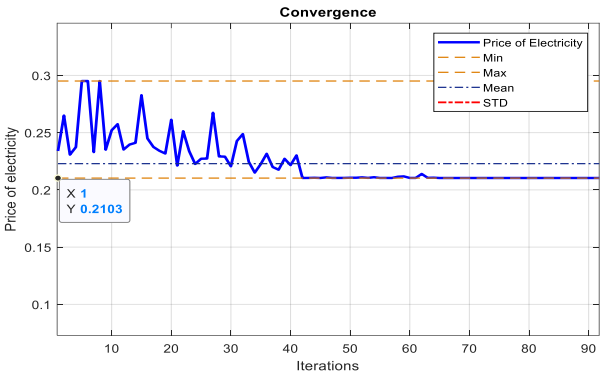

Figure 12 Variation of iteration vs price of electricity for PSO

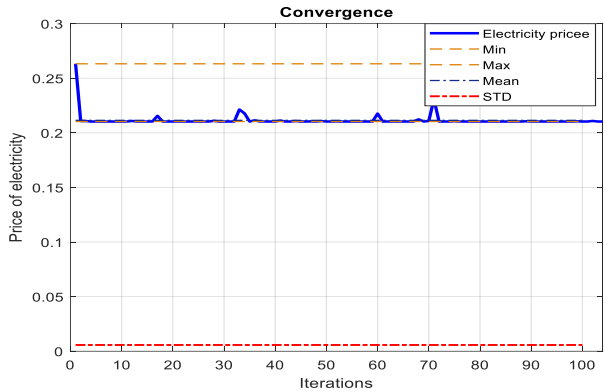

Figure 13 Variation of iteration vs price of electricity for GA

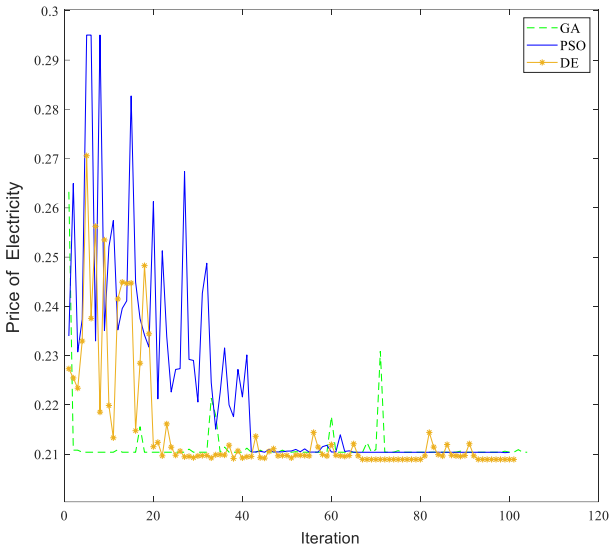

Figure 14 Price of electricity for DE, PSO and GA

4.4 Performance of the Algorithm

The convergence of the system determines the robustness of the system under study. Figure 15 shows the convergence of the improved DE algorithm simulated throughout the study with the lower bounds of [200 200] and upper bound of [1400 1400] for the PV panels and battery.

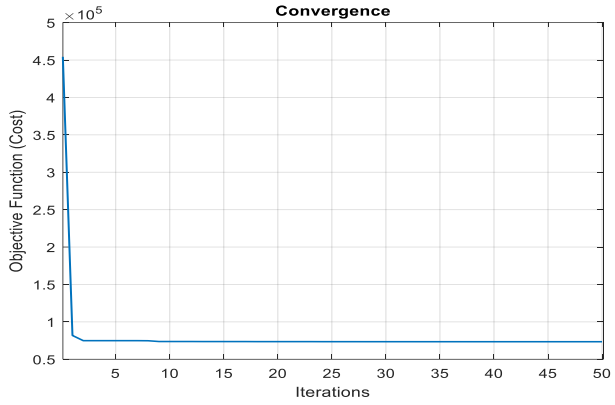

Figure 15 Convergence of the DE algorithm

The same bounds were selected for GA and PSO in the subsequent simulations. Figure 15 shows that the convergence of the improved DE algorithm is very fast and converges to the final solution in 50 iterations.

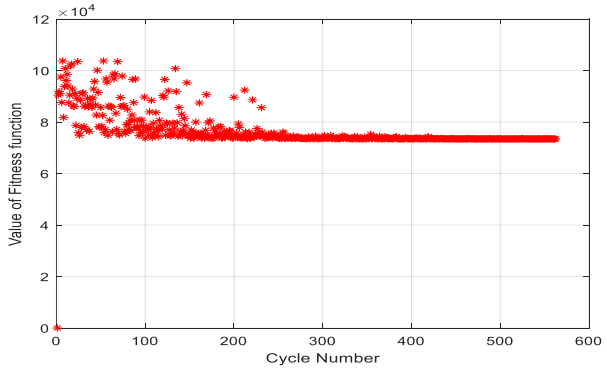

Figure 15 Fitness function of the DE algorithm

The fitness function of PSO and GA is shown in Figures 16 and 17 respectively. This simulation is conducted under Standard Test Conditions as a basis of comparison to the parent algorithm DE used in implementing the system under study. It could be seen that convergence of DE is approximately three times faster than GA, since the lower and the upper bounds are the same for the two algorithms. Comparing Figures 15 and 17, the DE converges at approximately 500 iterations and GA converges at 1800 iterations and that of PSO is 800 iterations. The GA, as a rule, executes faster if its fitness function is vectorized.

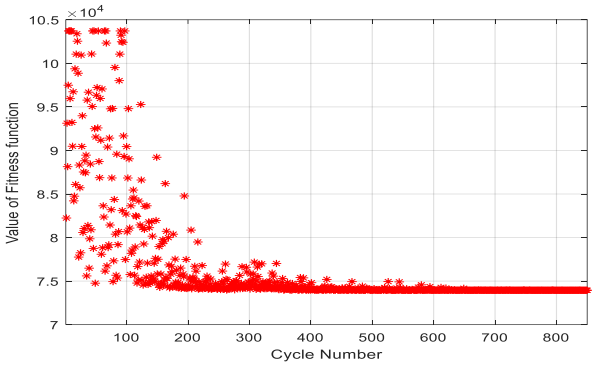

Figure 16 Fitness function of the PSO algorithm

This means that GA calls the fitness function only once, but expects the fitness function to register readiness for all individuals in the current population immediately [51]. For the nonlinear constraint function, the fitness function must recognize any number of columns to use vectorization. Through inheritance operations such as crossover and mutation, GA can converge and produce the fittest chromosome that has a higher wellness value at the end of the GA process.

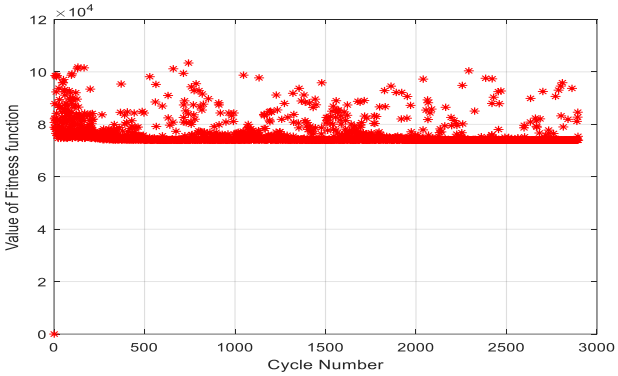

Figure 17 Fitness function of the GA algorithm

The raw fitness score is converted by fitness scaling that is returned by the fitness function values in an order that is reasonable for the selected function. The selected function utilizes the values of the scaled fitness to choose a higher probability of the selected individuals with esteem values. The scope of the scaled influences the performance of the GA, the scaled value shifts too broadly, and the individuals with the most elevated scaled value duplicate too quickly, assuming control over the populace genetics and keeping the hereditary

algorithms from looking through different territories of the arrangement space.

5.0 CONCLUSION

The optimal size of PV and battery storage Off-Grid PV system is a fundamental requirement for improving the efficiency and reliability of the system. In this project, improved DE was adopted for optimum sizing of the Off-grid PV system considering the uncertainties of the system. The hourly load demand and series data of Assin Bungalow as obtained from the Electricity Company of Ghana (ECG) and National Aeronautics and Space Administration (NASA) respectively are presented in the analysis.

The main goal of this project is to minimize the cost of installing the system and thereby reduce the price of electricity by determining the appropriate optimum number of PV modules and battery banks required for the case study. The proposed system's effectiveness was tested using improved DE, PSO and GA utilizing MATLAB algorithm carried out under desirable test conditions to specific advance changes in irradiance pattern and other uncertainties associated with the system.

The outline of various search ranges set for PV and Battery technologies and their objective function is presented. The impact of the control parameters setting and the influence of those for various algorithms have been analyzed. The result shows that DE offered the best optimal solution in terms of cost and convergence time.

The capacity of the storage battery is optimally selected to store energy when there is excess energy available, to provide when required, and to prevent instability during current and voltage transients.

The improved DE algorithm minimizes the premature convergence to local minima, associated with conventional metaheuristics algorithms. DE algorithm is more efficient as compared to PSO and GA algorithms and requires less computational time and memory for implementation as it converges faster. The result of the optimization shown in this project can be implemented to meet specific requirements. Analyzing the three fitness functions it could be seen clearly that the convergence rate of the DE is about 30% faster than PSO and far better than GA which means more computational time and memory are required for both PSO and GA.

Conflicts of Interest

The author(s) declare(s) that there is no conflict of interest regarding the publication of this paper.

Acknowledgement

This study is supported by the UTM Transdisciplinary Research Grant (TDRG) under cost center no. 06G48.

References

[1] C. Mekontso, A. Abdulkarim, I. S. Madugu, and O. Ibrahim. 2019. Review of Optimization Techniques for Sizing Renewable Energy Systems. *Computer Engineering and Applications Journal*. 8(1): 12-30. Doi: 10.18495/comengapp.v8i1.285.

[2] International Energy Agency. 2018. Global Energy & CO_2 Status Report. March. 1-15. [Online]. Available: http://www.iea.org/publications/freepublications/publication/GECO2017.pdf%0Ahttps://www.iea.org/publications/freepublications/publication/GECO2017.pdf.

[3] M. Isa, C. W. Tan, and A. H. M. Yatim. 2018. A Proposition of a Standalone Photovoltaic System for Educational Building in Malaysia. *Int. J. Renew. Energy Resour.* 8(1): 1-6.

[4] A. Askarzadeh and A. Askarzadeh. 2017. Optimisation of Solar and Wind Energy Systems : A Survey. 0750. Doi: 10.1080/01430750.2016.1155493.

[5] E. T. El Shenawy, A. H. Hegazy, and M. Abdellatef. 2017. Design and Optimization of Stand-alone PV System for Egyptian Rural Communities. 12(20): 10433-10446.

[6] M. Hafner, S. Tagliapietra, and L. de Strasse. 2018. Energy Investments for Africa's Energy. *Springer Briefs in Energy*. Doi: 10.1007/978-3-319-92219-5.

[7] V. Dabra, K. K. Paliwal, P. Sharma, and N. Kumar. 2017. Optimization of Photovoltaic Power System: A Comparative Study. *Prot. Control Mod. Power Syst*. 2(1): Doi: 10.1186/s41601-017-0036-2.

[8] M. Kamran *et al.* 2018. Designing and Optimization of Stand-alone Hybrid Renewable Energy System for Rural Areas of Punjab, Pakistan. *Int. J. Renew. Energy Res*. 8(4): 2385-2397.

[9] S. Kamali. 2016. Feasibility Analysis of Standalone Photovoltaic Electrification System in a Residential Building in Cyprus. *Renew. Sustain. Energy Rev*. 65: 1279-1284. Doi: 10.1016/j.rser.2016.07.018.

[10] F. Huneke, J. Henkel, J. A. B. González, and G. Erdmann. 2012. Optimisation of Hybrid Off-grid Energy Systems by Linear Programming. *Energy. Sustain. Soc*. 2(1): 1-19. Doi: 10.1186/2192-0567-2-7.

[11] E. T. El Shenawy, A. H. Hegazy, and M. Abdellatef. 2017. Design and Optimization of Stand-alone PV System for Egyptian Rural Communities. *Int. J. Appl. Eng. Res*. 12(20): 10433-10446.

[12] M. B. Eteiba, S. Barakat, M. M. Samy, and W. I. Wahba. 2018. Optimization of an Off-grid PV/Biomass Hybrid System with Different Battery Technologies. *Sustain. Cities Soc*. 40: 713-727.

[13] R. U. Islam, M. S. Hossain, and K. Andersson. 2020. A Learning Mechanism for Brbes using Enhanced Belief Rule-Based Adaptive Differential Evolution. *2020 Joint 9th International Conference on Informatics, Electronics & Vision (ICIEV) and 2020 4th International Conference on Imaging, Vision & Pattern Recognition (icIVPR)*, 2020. 1-10.

[14] P. Ouyang and V. Pano. 2015. Comparative Study of DE, PSO and GA for Position Domain PID Controller Tuning. *Algorithms*. 8(3): 697-711. Doi: 10.3390/a8030697.

[15] S. Gao, K. Wang, S. Tao, T. Jin, H. Dai, and J. Cheng. 2021. A State-of-the-art Differential Evolution Algorithm for Parameter Estimation of Solar Photovoltaic Models. *Energy Convers. Manag*. 230: 113784. Doi: 10.1016/j.enconman.2020.113784.

[16] Z. Huang. 2013. An Improved Differential Evolution Algorithm based on Statistical Log-linear Model. *Sensors and Transducers*. 159(11): 277-281.

[17] Y. Ma and Y. Bai. 2020. A Multi-population Differential Evolution with Best-random Mutation Strategy for Large-scale Global Optimization. *Appl. Intell*. 1-17.

[18] T. Sum-Im. 2009. A Novel Differential Evolution Algorithmic Approach to Transmission Expansion Planning.

[19] X. Zhong and P. Cheng. 2020. An Improved Differential Evolution Algorithm Based on Dualstrategy. *Math. Probl. Eng*. Doi: 10.1155/2020/9767282.

[20] R. A. Khanum, M. A. Jan, N. M. Tairan, and W. K. Mashwani. 2016. Hybridization of Adaptive Differential Evolution with an Expensive Local Search Method. *J. Optim*. 1-14. Doi: 10.1155/2016/3260940.

[21] M. B. Eteiba, S. Barakat, M. M. Samy, and W. I. Wahba. 2018. Optimization of an Off-grid PV/Biomass Hybrid System with Different Battery Technologies. *Sustainable Cities and Society*. 40: 713-727. Doi: 10.1016/j.scs.2018.01.012.
[22] T. M. N. T. Mansur, N. H. Baharudin, and R. Ali. 2018. Optimal Sizing and Economic Analysis of Self-consumed Solar PV System for a Fully DC Residential House. *2017 IEEE Int. Conf. Smart Instrumentation, Meas. Appl. ICSIMA 2017*. 2017(November): 1-5. Doi: 10.1109/ICSIMA.2017.8312006.
[23] W. M. Sarhan, A. N. Alkhateeb, K. D. Omran, and F. H. Hussein. 2006. Effect of Temperature on the Efficiency of the Thermal Cell. *Asian J. Chem.* 18(2): 982-990.
[24] S. Asumadu-Sarkodie and P. A. Owusu. 2016. A Review of Ghana's Solar Energy Potential. *Aims Energy*. 4(5): 675-696.
[25] P. Rajendran and H. Smith. 2016. Modelling of Solar Irradiance and Daylight Duration for Solar-powered UAV sizing. *Energy Exploration & Exploitation*. 34(2): 235-243. Doi: 10.1177/0144598716629874.
[26] Seyed Abbas Mousavi Maleki, H. Hizam, and Chandima Gomes. 2017. Estimation of Hourly, Daily and Monthly Global Solar Radiation on Inclined Surfaces: Models Re-Visited. *Energies*. 10(1): 134. Doi: 10.3390/en10010134.
[27] C. A. Gueymard. 2014. A Review of Validation Methodologies and Statistical Performance Indicators for Modeled Solar Radiation Data: Towards a Better Bankability of Solar Projects. *Renew. Sustain. Energy Rev.* 39: 1024-1034.
[28] S. Mousavi Maleki, H. Hizam, and C. Gomes. 2017. Estimation of Hourly, Daily and Monthly Global Solar Radiation on Inclined Surfaces: Models Re-Visited. *Energies*. 10(1): 134. Doi: 10.3390/en10010134.
[29] T. A. Olukan and M. Emziane. 2014. A comparative Analysis of PV Module Temperature Models. *Energy Procedia*. 62: 694-703. Doi: 10.1016/j.egypro.2014.12.433.stab.pdf.
[31] Martin Murnane and Adel Ghazel. A Closer Look at State of Charge (SOC) and State of Health (SOH) Estimation Techniques for Batteries. Analog Devices.
[32] P. Boonluk, S. Khunkitti, P. Fuangfoo, and A. Siritaratiwat. 2021. Optimal Siting and Sizing of Battery Energy Storage: Case Study Seventh Feeder at Nakhon Phanom Substation in Thailand. *Energies*. 14(5): Doi: 10.3390/en14051458.
[33] Diouf, B., Avis, C. 2019. The Potential of Li-ion Batteries in ECOWAS Solar Home Systems. J. Energy Storage. 22: 295-301. Doi:10.1016/j.est.2019.02.021.
[34] R. Dufo-López, T. Cortés-Arcos, J. S. Artal-Sevil, and J. L. Bernal-Agustín. 2021. Comparison of Lead-acid and Li-ion Batteries Lifetime Prediction Models in stand-Alone Photovoltaic Systems. *Appl. Sci.* 11(3): 1-16. Doi: 10.3390/app11031099.
[35] Z. Othman, S. I. Sulaiman, I. Musirin, A. M. Omar, and S. Shaari. 2017. Optimal Sizing Stand Alone Photovoltaic System using Evolutionary Programming. *ACM Int. Conf. Proceeding Ser.* Part F1278. 302-306. Doi: 10.1145/3057039.3057057.
[36] U. S. E. I. Administration. 2020. Levelized Cost and Levelized Avoided Cost of New Generation Resources in the Annual Energy Outlook 2016. *Us Eia Lcoe*. February: 1-20.
[37] S. Y. Yuen and X. Zhang. 2015. On Composing an Algorithm Portfolio. *Memetic Comput.* 7(3): 203-214.
[38] Bp Solar. 2009. Solar Energizer Series Owners Manual, Part number 2627.0116 – 0609R7. <www.bpsolar.com>.
[39] M. Rasid, J. Murata, and H. Takano. 2017. Fossil Fuel Cost Saving Maximization: Optimal Allocation and Sizing of Renewable-energy Distributed Generation Units Considering Uncertainty via Clonal Differential Evolution. *Appl. Therm. Eng*. 114: 1424-1432. Doi: 10.1016/j.applthermaleng.2016.10.030.
[40] M. A. A. M. S. Khalid. 2018. Seven-parameter PV Model Estimation using Differential Evolution. *Electr. Eng*. 100(2): 971-981. Doi: 10.1007/s00202-017-0542-2.
[41] B. Kazimipour, X. Li, and A. K. Qin. 2014. Effects of Population Initialization on Differential Evolution for Large Scale Optimization. *2014 IEEE Congress on Evolutionary Computation (CEC)*. 2404-2411. Doi: 10.1109/CEC.2014.6900624.
[42] I. Al Hamrouni, A. Khairuddin, and M. Salem. 2013. Application of Differential Evolution Algorithm in Transmission Expansion Planning. *Appl. Mech. Mater*. 394: 314-320. Doi: 10.4028/www.scientific.net/AMM.394.314.
[43] Y. Wu, W. Lee, and C. Chien. 2011. Modified the Performance of Differential Evolution Algorithm with Dual Evolution Strategy. *International Journal of Innovative Computing, Information & Control: IJICIC*. 8(4).
[44] S. Mandal and K. K. Mandal. 2020. Optimal Energy Management of Microgrids under Environmental Constraints using Chaos Enhanced Differential Evolution. *Renew. Energy Focus*. 34: 129-141. Doi: 10.1016/j.ref.2020.05.002.
[45] M. Centeno-telleria, E. Zulueta, U. Fernandez-gamiz, and D. Teso-fz-betoño. 2021. Differential Evolution Optimal Parameters Tuning with Artificial Neural Network. *Mathematics*. 9(4): 4271-20.
[46] M. Fei, S. Ma, X. Li, X. Sun, L. Jia, and Z. Su. 2017. Advanced Computational Methods in Life System Modeling and Simulation. *International Conference on Life System Modeling and Simulation, LSMS 2017 and International Conference on Intelligent Computing for Sustainable Energy and Environment, ICSEE 2017, Nan*. 761. Springer.
[47] T. Eltaeib and A. Mahmood. 2018. Differential Evolution: A Survey and Analysis. *Appl. Sci.* 8(10): Doi: 10.3390/app8101945.
[48] G. Hailu and A. S. Fung. 2019. Optimum Tilt Angle and Orientation of Photovoltaic Thermal System for Application in Greater Toronto Area, Canada. *Sustain.* 11(22). Doi: 10.3390/su11226443.
[49] Y. Tian and Y. Zhang. 2022. A Comprehensive Survey on Regularization Strategies in Machine Learning. *Inf. Fusion*. 80: 146-166.
[50] D. Akinyele. 2017. Battery Storage Technologies for Electrical Applications : Impact in Stand-Alone Photovoltaic Systems. *Energies.* 10(11). Doi: 10.3390/en10111760.
[51] J. Dias, H. Rocha, B. Ferreira, and M. do C. Lopes. 2014. A Genetic Algorithm with Neural Network Fitness Function Evaluation for IMRT Beam Angle Optimization. *Cent. Eur. J. Oper. Res.* 22(3): 431-455.